Maaß et al. 2012, Influence of the dispersed phase fraction on experimental and predicted drop size distributions in breakage dominated stirred systems, Chem. Eng. Sci., DOI: 10.1016/j.ces.2012.03.050

INFLUENCE OF THE DISPERSED PHASE FRACTION ON EXPERIMENTAL AND PREDICTED DROP SIZE DISTRIBUTIONS IN BREAKAGE DOMINATED STIRRED SYSTEMS

Sebastian Maaß[1*], Niklas Paul[1], Matthias Kraume[1]

[1]Technische Universität Berlin, Straße des 17. Juni 135, Sekr. MA 5-7, 10623 Berlin, Germany

[*]corresponding author (sebastian.maass@tu-berlin.de)

ABSTRACT

The effect of the dispersed phase fraction on the evolving drop size distribution in different low viscous agitated liquid/liquid systems was investigated. The analysis focused on the drop breakage phenomena by hindering the coalescence completely. Therefore, polyvinyl alcohol concentrations were used around three times higher than the critical micelle concentration.

The measured drop sizes were increasing with increasing dispersed phase fraction. As coalescence was completely hindered and also the measured dispersion viscosity showed no influence on the dispersed phase hold-up, the size increase is proposed to be a result of turbulence hindering.

The influence of the dispersed phase fraction on the drop sizes in breakage dominated systems was well reproduced with population balance equation (PBE) simulations. The used breakage models require a turbulence damping factor ($1+\varphi_d$), which is used in most of the common models. Summarizing the various PBE simulations we can conclude that drop sizes in systems with different dispersed phase fractions can be easily predicted, if the model parameters are fitted to one set of experiments studying the same physical system. The change of the solvent was successfully simulated with outstanding results for two of the three further investigated organics.

The used Weber correlations were also able to reproduce the linear interdependency between the drop size and the dispersed phase fraction. Unfortunately, every change in the dispersed phase needed new parameter estimation. As at least three out of four different liquid/liquid systems were predicted with excellent results, the PBE is proposed as a more robust tool which gives additionally information about the transient behavior of the system. Therefore, PBE should be used rather than the classical correlations widely used in academics and industries.

KEYWORDS:

Drop size prediction, drop size distribution, population balance equation, liquid/liquid dispersion, hold-up, phase fraction, drop breakage, stirred tank

1 INTRODUCTION

Stirred liquid/liquid systems are used in a large variety of technical processes, with major importance for chemical, pharmaceutical, mining, petroleum and food industries. In these systems, two immiscible liquids are mixed with each other, so that one phase is dispersed into the other one.

The description of these dispersion processes is very complex, because the opposed phenomena of drop breakage and coalescence have to be considered. These are the main influencing factors on the drops sizes and therewith on the interfacial area. For an exact prediction of heat and mass transfer and reaction rates in liquid/liquid systems, exact knowledge of the interfacial area is required.

The dispersed phase hold-up, also named the dispersed phase volume fraction φ_d, is a significant parameter for process intensification (Sengupta et al. 2006). An increase of the dispersed phase can increase the interfacial area and therewith intensify extraction processes significantly. In polymerization reactions the dispersed phase fraction is equivalent to the productivity of the process. Every increase in dispersed phase is an increase in reactor capacity, if the size requirements on the particles are fulfilled. Another example from biotechnology is a two-phase biotransformation process. These systems are using the help of an organic phase to facilitate the dissolution of high substrate concentrations. So the increase in dispersed hold-up increases the space-time yield of the process (Cull et al. 2001).

Literature states clearly that an increase in the dispersed phase fraction causes the mean drop diameters to increase. Razzaghi and Shahraki (2010) summarize the reported interpretation of this influence scheme as follows: a number of authors attribute this behavior to turbulence damping (Brown and Pitt 1972; Cohen 1991; Doulah 1975) while others ascribe it mainly to coalescence (Delichatsios and Probstein 1976). Furthermore, some authors believe that both coalescence and turbulence dampening are equally responsible for the observed trends (Angle and Hamza 2006a; Gäbler et al. 2006; Godfrey et al. 1989).

Doulah (1975) correlated the drop size decrease by an increase in dispersion viscosity, expressed by the Einstein equation (Einstein 1906; Einstein 1911) and not to turbulence damping in the continuous phase. This slight but important difference may be a third reason for drop size increase with increasing dispersed phase fraction.

Only a few workers reported the opposite in drop size behavior. Cho and Kamal (2002) were analyzing the drop size in polymer blends with high viscosity ratios. These authors state that the deformation rate increases with rising volume fractions of the dispersed phase, and the shear stress also increases, leading to an increase of the breakup. The total deformation of the dispersed phase increases with increasing volume fractions, resulting in a decrease of the size of the dispersed phase particles. So the whole field is still open to question.

This work focuses on the analysis of the effect of dispersed phase fraction on drop breakage. Therefore, four different liquid/liquid systems without any coalescence have been investigated. Liquid/liquid dispersions in industry are rarely ‘clean’, with ‘additional material’ either being unwanted (unknown) but present, or deliberately added. Such an additive or unintended ‘impurity’ can have a profound impact on the structure of the dispersion, leading even to a completely stabilized dispersion (Nienow 2004). A surfactant is used in this study to completely hinder coalescence and stabilize the dispersion. These circumstances allowed for a system analysis under pure breakage conditions. The experiments have been carried out to determine the influence of the dispersed phase fraction on the transient evolution of the drop size distributions.

The main goal of this study is to evaluate and further develop the prediction capacities for evolving liquid/liquid dispersions under the influence of the dispersed phase fraction. Therefore, pre-

diction correlations, based on Hinze's theory (Hinze 1955) and population balance models from literature, are introduced in section 2 and 3. Section 4 presents the experimental and computational methods that were used. The results of the work are demonstrated and discussed in section 5. Finally section 6 sums up the main conclusions drawn from this study.

2 MEAN DROP SIZE PREDICTION AND PREVIOUS EXPERIMENTAL WORK

Owing to the immense industrial importance of liquid/liquid dispersions, several studies on experimental measurements of drop size distributions in stirred tanks have been reported in literature. An excellent literature survey, which allows detailed comparison of existing experimental work and correlation approaches is given by Singh et al. (2008). They review the research of more than five decades and compare them with their own experimental results. Also the work of Angle and Hamza (2006b) is recommended as a valuable introduction into the field of liquid/liquid dispersion modeling and experimental analysis. In most of the cases, the experimental data have been correlated using the functional form developed by Hinze (1955) ($d_{32} \sim We^{-0.6}$) and modified by various authors into the following general form:

$$\frac{d_{32}}{D} = C_1(1 + C_2 \cdot \varphi_d)We^{-0.6},\ We = \frac{\rho_c n^2 D^3}{\gamma} \tag{1}$$

Here We is the Weber number which is the ratio of the disrupting force due to turbulence to the restoring force due to interfacial tension. Equation (1) was extended by including the viscosity aspects. The work of Calabrese et al. (1986) is especially recommended as a valuable study on this influence parameter. These authors introduced the viscosity vessel number Vi into the correlation:

$$\frac{d_{32}}{D} = C_1(1 + C_2\varphi_d)We^{-0.6} \cdot (1 + C_3(1 - C_4\varphi_d)Vi)^{0.6};\ Vi = \frac{\eta_d}{\sqrt{\rho_d \cdot \gamma \cdot D}} \tag{2}$$

Although this approach takes more physical properties into account, it also introduces a third correlation parameter C_3. This drawback leads to a huge range of various parameter combinations used in the literature (see Angle and Hamza 2006b; Pacek et al. 1998; Singh et al. 2008; Zerfa and Brooks 1996 for a parameter overview). Only a few additional experimental works will be added in the following paragraphs to complete the review list from these author groups.

Scott et al. (1958) studied the effect of dispersed phase fraction on the interfacial area in an orifice mixer. The area was increasing with rising hold-up, although the drop size increased too. Okufi et al. (1990) analyzed the influence of the dispersed phase fraction on different scales in a stirred tank. They reproduced the drop size increase for a hold-up increase in all investigated tank sizes. Kraume et al. (2004) studied the influence of dispersed phase fraction for strong coalescing liquid/liquid systems in a standard stirred tank. They analyzed an anisole/water, butyl acetate/water and a toluene/water system in the range of $0.05 \leq \varphi_d \leq 0.5$. They found increasing mean diameters for increasing dispersed phase fractions. Additionally they stated that the influence of the phase fraction on the mean diameter decreases for rising phase ratios.

The latest studies, as known to the authors, explicitly analyzing the influence of the hold-up on the drop size are the works of El-Hamouz (2009) and Khakpay and Abolghasemi (2010). Both publications show a linear relation between the mean diameter and the dispersed phase fraction. This is also true for the works of Gäbler et al. (2006). These authors investigated a toluene/water

system with low coalescence at high pH values. They again determined a linear correlation between the mean diameter and the dispersed phase fraction in their experiments and simulations using the population balance equation. Unfortunately, the simulations failed to reproduce the experimental results quantitatively. Gäbler et al. (2006) assumed that the breakage is disproportionately high taken into account compared with the coalescence modeling. So they concluded that the "dampening factor" of the turbulent energy dissipation (ε is damped by the inverse factor of $(1+\varphi_d)$ – see also following section) does not properly reflect the system change.

3 POPULATION BALANCE EQUATION

This section will describe the modeling ideas behind the population balance equation (PBE). Additionally four different breakage models used in the PBE will be introduced. In order to be able to simulate the evolution of a size distribution, suitable models should be used in the population balance. Therefore, this study provides an evaluation and also further developments of existing breakage models.

3.1 Formulation for breakage dominated systems

The PBE in a batch reactor can be expressed as a univariate PBE, which only considers size change of the individuals:

$$\frac{\partial f(V_p)}{\partial t} = B_b(V_P,t) - D_b(V_P,t) + B_c(V_P,t) - D_c(V_P,t) \tag{3}$$

Here B_b, D_b, B_c and D_c are the birth rate by breakage, death rate by breakage, birth rate by coalescence, and death rate by coalescence, respectively. While the coalescence efficiency is assumed to be zero in this work only the breakage associated terms are used. This major simplification is verified with experimental findings which are later discussed in this study. The birth and death terms are described as follows:

$$\frac{\partial f(V_p)}{\partial t} = \int_{V_p}^{V_{P,max}} \nu(V_p')\beta(V_p,V_p')g(V_p')f(V_p',t)\,dV_P - g(V_p)f(V_p,t) \tag{4}$$

where $g(V_P)$ is the breakage frequency, $\nu(V_P)$ is the number of dispersed fluid entities formed upon breakage of a particle V_P, and $\beta(V_P,V_P')$ is the size distribution of daughter fragments formed from the breakage of a particle V_P. A more detailed discussion of the population balance in general can be found in Ramkrishna (2000).

Considering a highly inhomogeneous energy dissipation rate ε in a stirred tank and the dependence of the drop size distribution on the energy dissipation rate, a detailed description of the flow field is needed. A fully predictive model that will solve the discretized population balance equations along with the flow and turbulence equations on a fine grid demands exorbitant computational domain. The number of equations to be solved will be very large as there will be one equation for each drop class. A simplification can be achieved by solving the flow equation on a fine grid followed by solution of population balance equations on a very coarse grid (Singh et al. 2008). Coarse may mean down to only two zones, where one zone stands for the impeller region and one for the bulk region in the vessel. Some studies using this simplified approach with varying number of zones have been reported (Alexopoulos et al. 2002; Alopaeus et al. 2002; Alopaeus et al. 2009; Maaß et al. 2010). This work follows the two-zone modeling approach.

3.2 Application of different models for the breakage rate

A profound overview of existing model approaches for the breakage rate, also called breakage frequency, is given by Liao and Lucas (2009). They state overall that models should be based on physical observations and validated properly against experimental data. That was already the aim of several studies evaluating PBE breakage kernels based on experimental studies (Gäbler et al. 2006; Patruno et al. 2009; Ruiz and Padilla 2004; Singh et al. 2009). As already mentioned, Gäbler et al. (2006) studied the influence of the dispersed phase fraction for a low coalescing system. Two different breakage rates have been used by them (Alopaeus et al. 2002; Coulaloglou and Tavlarides 1977). Both breakage rates failed within the PBE approach to predict the change in the drop size by changing the hold-up quantitatively right. However, the still coalescing system also required the use of coalescence kernels within the model approach. Therefore, a clear judgment about the quality of the model based on the coalescence or the breakage submodels of the population balance is impossible.

Patruno et al. (2009) considered only breakage processes within their description of the population balance. Four different breakage kernels were used by them. The phenomenological models by Coulaloglou and Tavlarides (1977) and Martínez-Bazán et al. (1999), two breakage kernels derived from inverse problems, Sathyagal and Ramkrishna (1996), and an own developed kernel , derived from inverse problems. One set of experimental data was used for the evaluation of all the simulation results. The model of Martínez-Bazán et al. (1999) failed in the evaluation process but the other three kernels were able to reproduce the experimental data in an acceptable range after parameter fitting. However, Patruno et al. (2009) still asked the question for the physically most meaningful kernel without being able to answer it. Additionally, it is to be remembered that any breakage kernel obtained with an inverse problem technique will be problem dependent and will be accurate only for the same experimental conditions from which it was derived (Patruno et al. 2009). Therefore, only phenomenological breakage rates are evaluated in this study. The four different breakage rates, used in this work, are introduced in the following paragraphs.

3.3 Breakage rate models used in this study

The most widely used and quoted model is the approach of Coulaloglou and Tavlarides (1977). Further, this model constituted the basis from which most of the breakage models in turbulent flowing liquid/liquid dispersions were derived (Azizi and Al Taweel 2011). It assumes that both phases are moving at the same velocity in a locally homogeneous isotropic turbulence field (Azizi and Al Taweel 2010). A drawback of this model is the assumption of negligible viscous effects, as can be seen in the following equation:

$$g(d_p) = c_{1,b}\,\frac{\varepsilon^{1/3}}{(1+\varphi_d)\,d_P^{2/3}}\exp\left(-c_{2,b}\,\frac{\gamma(1+\varphi_d)^2}{\rho\varepsilon^{2/3}d_P^{5/3}}\right) \tag{5}$$

After studying breakage time modeling, Maaß and Kraume (2012) were contrasting this assumption of negligible viscous effects by experimental data based on single drop experiments. A new breakage time correlation was derived (see Maaß and Kraume 2012 for details). The inverse of the breakage time is connected with the breakage probability following Coulaloglou and Tavlarides (1977):

$$g(d_p) = c_{1,b}\,\frac{\dot{\varepsilon}}{n}\left(\ln\frac{d_P\dot{\varepsilon}\eta_d}{\gamma Ca_{d,crit}}\right)^{-1}\frac{\varepsilon^{1/3}}{(1+\varphi)d_P^{2/3}}\exp\left(-c_{2,b}\,\frac{\gamma(1+\varphi_d)^2}{\rho_d\,\varepsilon^{2/3}d_P^{5/3}}\right) \tag{6}$$

The breakage rate is increasing for increasing drop diameter, reaches its maximum at a critical value and starts to decrease for larger drop sizes. Thus it is giving more stability to the larger drops. This kind of development was generally criticized by several authors (Chen et al. 1998; Ruiz and Padilla 2004; Tsouris and Tavlarides 1994) as inappropriate.

Alternatively, monotone increasing models are also used in this study. Alopaeus et al. (2002) developed a model based on the breakage rate by Narsimhan et al. (1979). They additionally included viscous effects in their model, based on the Voigt model which was originally proposed by Arai et al. (1977).

$$g(d_p) = c_{1b}\varepsilon^{1/3}\cdot\operatorname{erfc}\left(\sqrt{\frac{c_{2,b}\gamma}{\rho_c d_P^{5/3}\varepsilon^{2/3}}+\frac{c_{3,b}\eta_d}{\sqrt{\rho_c\rho_d}\,d_P^{4/3}\varepsilon^{1/3}}}\right) \tag{7}$$

Attending the pre-erfc term, no influence of the particle diameter is considered which leads to a monotone increasing breakage rate.

3.4 Model extension of the work by Alopaeus et al. (2002)

Experimental and numerical analysis of the turbulent flow field by Galinat et al. (2007) assume a damping effect of dispersed phases on the turbulence. Al Taweel and Landau (1977) have already introduced a simple model describing the selective dampening of the intensity of high-frequency eddies by introducing a dispersed phase into a continuous jet. This is in agreement with interpretation of Cohen (1991) who detected an increase in the minimum drop diameter measured with increasing dispersed phase fraction. As the smallest detected drop diameter can only be produced by breakage, a damping of the drop breakage is assumed. So they concluded that the influence of an increasing hold-up on coalescence is secondary compared to the influence of drop breakage.

To account for this dampening of the turbulence due to the dispersed phase fraction, the above equation could be written as:

$$g(d_p) = c_{1b}\,\frac{\varepsilon^{1/3}}{(1+\varphi)}\cdot\operatorname{erfc}\left(\sqrt{\frac{c_{2,b}\gamma\,(1+\varphi)^2}{\rho_c d_P^{5/3}\varepsilon^{2/3}}+\frac{c_{3,b}\eta_d\,(1+\varphi)}{\sqrt{\rho_c\rho_d}\,d_P^{4/3}\varepsilon^{1/3}}}\right) \tag{8}$$

While the original equation is only slightly extended, this model approach will be called extended Alopaeus in this work.

4 MATERIAL AND METHODS

The aim of this investigation is to analyze the influence of the dispersed phase fraction on the breakage behavior in different liquid/liquid system. Therefore, the emulsions were stabilized so no coalescence could occur. The four different organics used in this study vary in interfacial tension, density and viscosity. PBE models from literature have been used to predict the measured system behavior. While no coalescence was measured, only the breakage kernels have been used for the simulations.

4.1 Experimental set-up

Figure 1 and Table 1 show the main features of the selected stirred vessel, used for the drop swarm experiments. All geometrical parameters were kept constant for all experiments. A flat blade impeller was chosen for the dispersion experiments. The diameter ratio of D/T = 0.6 and a blade thickness of 0.02·D were kept constant for all experiments. The stirrer height h_{St} was 0.06·D. The clearance between stirrer and vessel bottom h was 1.8·D.

Table 1 – dimensions of the used stirred tank

T	H/T	l_B/T	D/T	h/D	h_{St}/D	w_B/T	Ne
155 mm	1.4	1.0	0.6	1.8	0.06	0.08	0.21

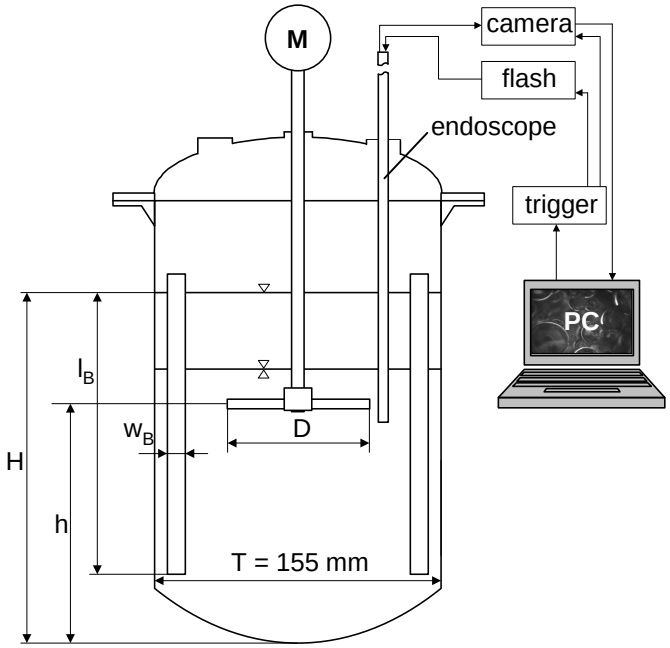

Figure 1 – experimental set-up and dimensions of the stirred tank

4.2 Measurement procedure

Four different organic solvents were used as dispersed phase: anisole, cyclohexane, n-butyl chloride and toluene. The used purities were always ≥ 99.98 %. To avoid coalescence in the dispersion experiments, high concentrations of polyvinyl alcohol (PVA) have been used. The degree of hydrolysis (72%) and the molecular weight (3586 g/mol) were kept constant for all experiments. The emulsion was stabilized with 3 mg of PVA per used 1 g of dispersed phase. The CMC was determined by analyzing the development of the interfacial tension over the surfactant concentration. Two methods have been used to determine the interfacial tension. The first was the pendant drop method (Jon et al. 1986) carried out on a Data Physics OCA 20. Additionally the interfacial tension was measured with a KRÜSS surface tensiometer Model K10 using the ring method. Both methods were in good agreement for the steady state values.

While all PVA concentrations are less than 10 mg/g, the physical properties of the continuous phase did not significantly vary from those of pure water (Chatzi et al. 1991). The physical prop-

erties of the four chemicals used as dispersed phases are presented in Table 2. The interfacial tensions for the pure component with deionized water determined in this study are presented. They are compared with literature values together with the measured influence of the PVA on the interfacial tension. Additionally the values for the densities and the viscosities are given.

Table 2 – physical properties of the investigated chemicals, own results and literature values

	interfacial tension γ [mN/m]			ρ [kg/m³] at 20°C	η_d [mPa·s] at 20°C
	c_{PVA} = 0 mg/g		c_{PVA} = 3 mg/g		
	own study	literature value	own study		
n-butyl chloride	37.1	37.1[i]	4.5	886	0.427[ii]
toluene	35.7	36.1[iii]	4.4	866	0.552[iv]
anisole	24.4	25.2[v]	3.8	996	1.017[vi]
cyclohexane	51.5	50.2[vii]	9.8	774	1.151[viii]

The influence of φ_d on the dispersion viscosity was analyzed only for the n-butyl chloride/water system using a viscometer Haake VT 550. The torque and rotational frequency of the attached stirrer were measured but showed no increase of torque at constant stirrer speed for increasing dispersed phase fraction. The system rather showed a decrease of the torque for increasing dispersed hold-up due to the decrease in dispersion density.

The transient drop size distributions (DSD) are determined using an in-situ photo optical method (Maaß et al. 2011a). It allows real time recording of 2D images of the particles. A measurement for particles in the size range of 5 to 5000 µm is provided. The technical details of the probe are described by Maaß et al. (2011a). The drop images are processed and analyzed fully automatically (Maaß et al. 2012). In order to ensure robust and accurate particle detection, every series of images is first pre-filtered to remove irrelevant and misleading image information. The subsequent particle recognition consists of three steps: Pattern recognition by correlation of pre-filtered grey values with search samples, the pre-selection of plausible circle coordinates, and the classification of each of those circles by an exact edge examination. The software employs a normalized cross correlation procedure algorithm. Manual evaluation of the drops on the images was

[i] Glass (1971)

[ii] Anson et al. (2005)

[iii] Misek et al. (1985)

[iv] Misek et al. (1985)

[v] Rashidnia et al. (1992)

[vi] Al-Jimaz et al. (2005)

[vii] Girifalco and Good (1957)

[viii] Wei and Rowley (1984)

used to quantify the accuracy of the image algorithm software. The details of the used algorithm are given by Maaß et al. (2012).

The mixing procedure was the same for every experiment. After the filling of the vessel with water and the pure organic compounds, the stirring started. After one minute of premixing, the surfactant was added and the time presented for the dispersion experiment started.

To evaluate the coalescence behavior under the selected conditions, the liquid/liquid system was first dispersed at 410 rpm. After 1 h of mixing the stirrer speed was immediately decreased to 250 rpm and the drop size was still measured, following instructions from literature (Raikar et al. 2009). An overview of the investigated dispersed phase fraction for the four different liquid/liquid systems is given in Table 3.

Table 3 – overview of the measurement program analyzing the four liquid/liquid systems

φ [%]	2	5	10	17	20	25	33	38	45
anisole	-	x	x	x	x	-	-	-	-
cyclohexane	-	x	x	-	x	-	-	-	-
toluene	-	x	x	x	x	-	x	-	x
n-butyl chloride	x	x	x	x	x	x	x	x	-

4.3 Numerical scheme

The Population Balance Equation is applied with the intention to calculate the transient drop size distribution in the stirred liquid/liquid system. A major result from previous studies is the necessity for the use of a two-zone model to meet the needs occurring with the extreme inhomogeneity of the energy dissipation in agitated reactors (Alopaeus et al. 2009; Maaß et al. 2010). Therefore, only the two-zone modeling approach was considered for simulations of drop sizes in the investigated vessels. One zone describes the stirrer region with high energy dissipation rates. The second zone describes the bulk region, which is the large region outside the stirrer region with very low dissipation rates. The ratio of $\varepsilon_{stirrer}/\varepsilon_{bulk} = 2.4 \cdot 10^3$ means that 95% of the power is dissipated in 3% of the reactor volume. The absolute values for the dissipation rates, the size of the zones and the volume flows between the two zones have been calculated using Computational Fluid Dynamics, these simulations have been verified using particle image velocimetry measurements (see Maaß et al. 2011b; Maaß et al. 2011c for details).

In order to solve the transient PBE, the commercial numerical solver PARSIVAL® (Particle Size Evaluation) is used (Wulkow et al. 2001). This code uses the Galerkin h-p method with a very efficient and adaptive discretization of drop size and time. In every time step the size distribution and the next time step is discretized adaptively. Submodels for the breakage rate and the daughter drop size distribution can be freely defined and an initial drop size distribution needs to be provided.

Based on the experimental results of the transient drop sizes, no coalescence kernel was taken into account for the simulations. Different breakage rates have been tested and are always com-

bined with a bimodal daughter drop size distribution (DDSD). The number of daughter drops ν is set to two, based on previous experimental studies (Maaß et al. 2007). The mother drop V_p breaks into two unequal sized daughter drops with a maximum probability of 1/6 V_p for the first and 5/6 V_p for the second daughter drop. This kind of DDSD has also been a result in a former study (Maaß et al. 2011d). In the simulations drop diameters were assumed to range between 1 and 10000 µm, with the upper limit being far above the maximum drop diameter observed in the experiments. An experimentally determined distribution from a toluene/water system was used as initial distribution for all simulations.

The free parameters in the used breakage rates have been estimated using PARSIVAL®. This estimation uses a damped Gauss-Newton method to minimize the differences between calculated and experimental values of the Sauter mean diameter ($d_{32} = \Sigma\ d_i^3/\Sigma d_i^2$) for every measured time step. The coefficient of determination R^2 describing the deviations between experiments and simulations has been maximized for each model.

5 RESULTS AND DISCUSSION

5.1 Interfacial tension

The exact knowledge of the interfacial tension in the used liquid/liquid systems is of great importance for the simulations of the drop size distributions. Furthermore the measurements of the interfacial tension depending on the PVA concentration provide essential information of the coverage of interfacial active molecules (PVA molecules) at the liquid/liquid interface. In this work a breakage dominated system shall be observed, hence a complete coverage is needed to hinder the coalescence completely.

The interfacial tension was measured for different PVA concentrations (0-3000 ppm). The time the PVA molecules need to adsorb at the interface has to be considered. Therefore, pendant drop measurements have been carried out. The interfacial tension of a droplet of a certain volume was observed for a definite time. For high surfactant concentrations the time that the system needed for reaching the steady state is reduced (Chatzi and Kiparissides 1995).

The experimental results of the interfacial tension measurements at the steady state for the systems n-butyl chloride/water and for cyclohexane/water are shown in Figure 2. This diagram shows the interfacial tension plotted against the logarithmic concentration of the PVA in the aqueous phase. For low PVA concentrations the interfacial tension decreases linearly. Increasing the PVA concentration causes specifically an increase of the PVA concentration at the liquid/liquid interface; hence the interfacial tension decreases (Hoffmann and Ulbricht 1995). After exceeding a specific concentration (CMC) where the interfacial tension hardly decreases, the equilibrium interface concentration is reached, so the interfacial tension remains constant. To identify this specific concentration in Figure 2, the distinct point of bending has to be found. Therefore, the dotted lines (best fitting lines) are plotted into this diagram. For both systems two bending points are observed in Figure 3. The first bending point is the more distinctive one and represents the CMC. As expected the CMC shifts to smaller concentrations in liquid/liquid systems compared to liquid/air systems (Hoffmann and Ulbricht 1995). In the liquid/air system a CMC of 40 µg/g was determined. There is an excellent agreement with the results of the interfacial tension of the n-butyl chloride/water system measuredby Chatzi and Kiparissides 1995).

Table 4 - Results for the CMC of the used systems related to the aqueous phase.

dispersed phase	anisole	cyclohexane	n-butyl chloride	toluene
CMC [µg/g]	1.69	2.01	2.47	2.59

The absolute values for the CMC concentrations related to the aqueous phase are given in Table 4. Note that the PVA concentrations are constant for the drop size experiments for the whole study. They are related to the organic phase. To avoid coalescence and to minimize the time dependency of the interfacial tension also for small dispersed phase fractions, a PVA concentration of 3000 ppm (3 mg PVA/g dispersed phase) is used for the next experiments.

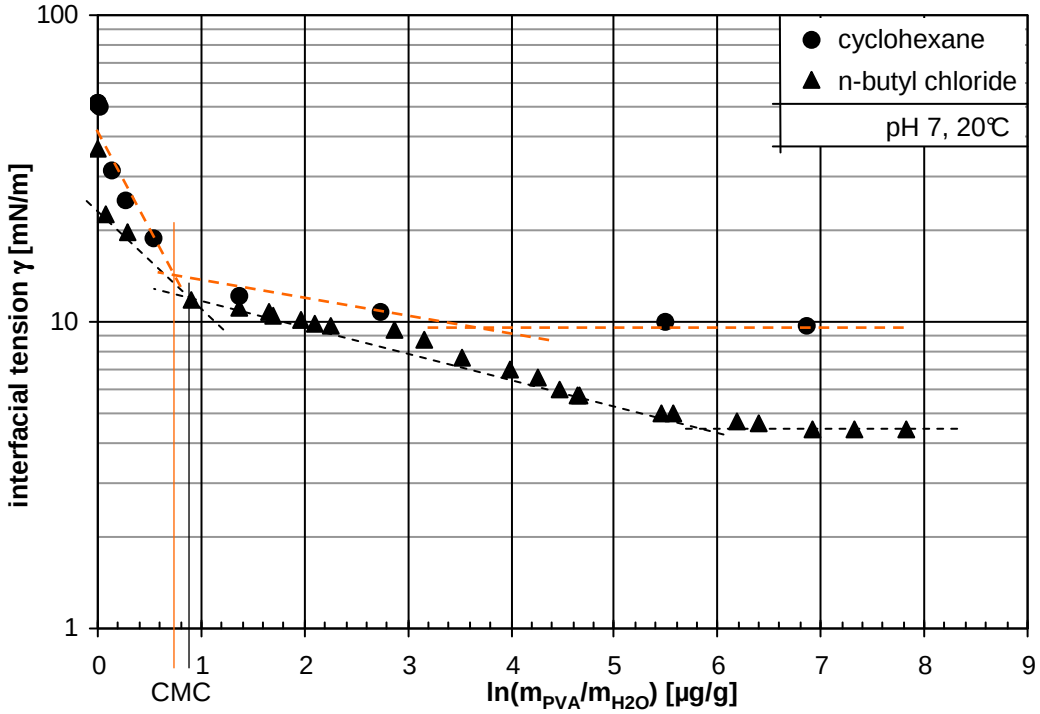

Figure 2 – interfacial tension of cyclohexane/water and n-butyl chloride/water as a function of the surfactant concentration

5.2 PBE parameter estimation

One set of experiments was used to determine optimum parameters within the four different breakage rates. The system used is toluene/water with a dispersed phase fraction of 17%, stabilized with 3 mg/g PVA, continuously agitated at 410 rpm with the already introduced flat blade impeller.

Note that the model by Coulaloglou and Tavlarides (1977) and the extended model by Maaß and Kraume (2012) contain two adjustment parameters ($c_{1,b}$, $c_{2,b}$ in equation (5) and (6)), whereas the model of Alopaeus et al. (2002) and also its extended form used in this study contain three parameters ($c_{1,b}$, $c_{2,b}$ and $c_{3,b}$ in equation (7) and (8)). The third parameter in these two model ver-

sions was set to $c_{3,b} = 2 \cdot 10^{-1}$. This is the recommended value by the authors obtained after sincere parameter estimation studies for different systems (Alopaeus et al. 2002). The parameter $c_{3,b}$ is dimensionless.

The values for the two other parameters have been estimated by minimizing the difference between one experiment and the simulation. To emphasize the transient behavior represented by the models, the experiment was carried over 19.5 hours. The drop size distributions have been measured after minute 1, 3, 5, 10, 15, 25, 40, 60, 80, 120, 180, 300, 550 and 1170. The permanent but smooth decrease in drop size over this agitation time forces the model into optimized values for $c_{1,b}$ and $c_{2,b}$. The magnitude of the decrease in the beginning of the process is mainly affected by $c_{1,b}$ while the running out of the simulation is foremost affected by $c_{2,b}$. Long term experiments value the influence of both parameters on the simulation results equally. The optimization procedure was stopped after achieving a value for the coefficient of determination R^2 larger than 0.98.

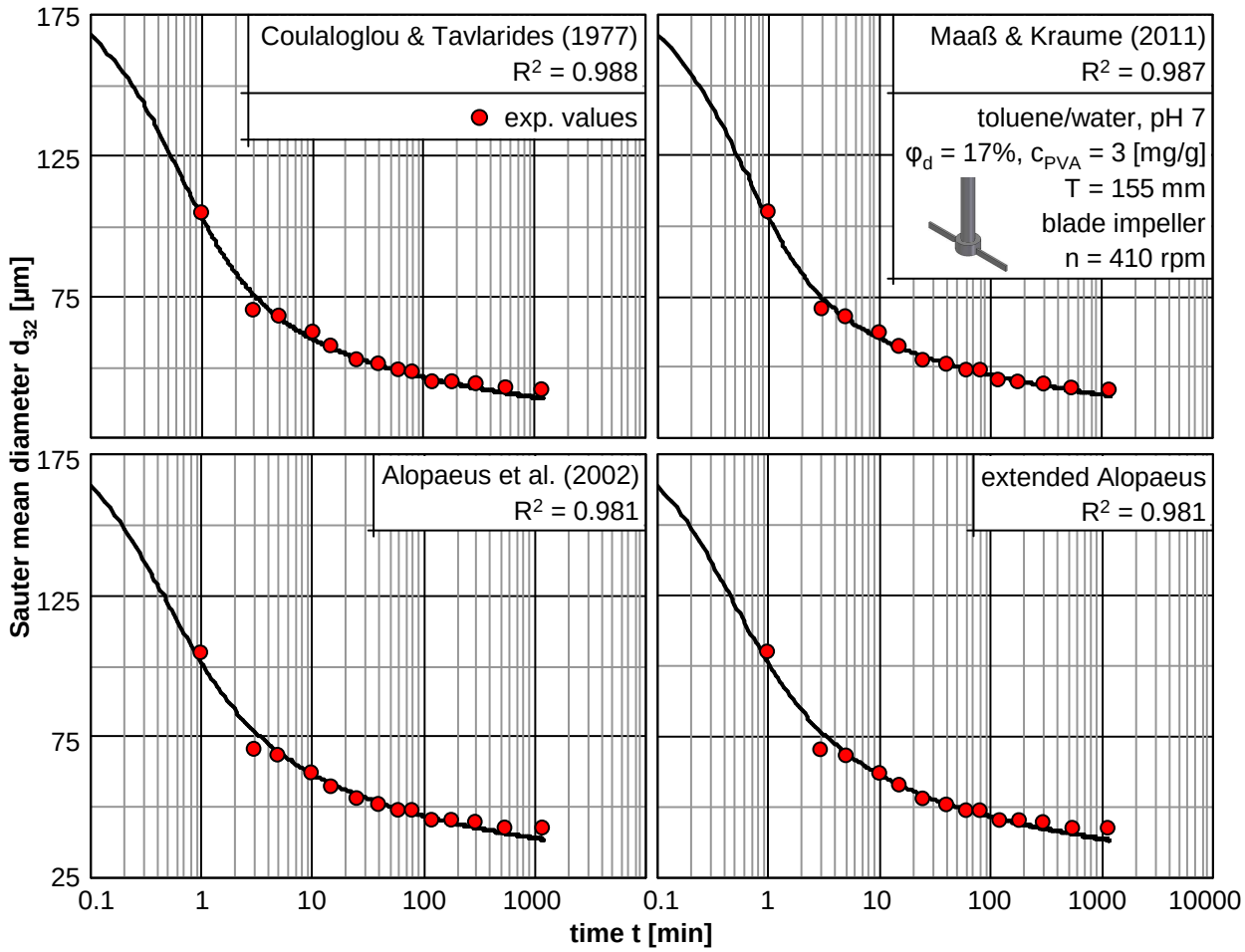

Figure 3 – simulated transient Sauter mean diameter for four different breakage rates after parameter estimation, compared with experiments

In Figure 3 the experimental results for the transient Sauter mean diameter over 1170 min of agitation are shown. They are compared with the simulation results achieved with four different PBE model approaches after parameter optimization. All four approaches reflect the transient behavior

excellently. Although the coefficients of determination for the simulations with the extended Alopaeus (including φ_d) and the original model by Alopaeus et al. (2002) are a little lower compared to the other two results, all are very satisfying. Even the natural scattering by experimental results does not lead to a single deviation larger than 9%. As can be seen from Figure 3 these deviations result from the value of d_{32} at minute 3. All other deviations between experiments and simulation are always below 5%, very often even below 1% (see also the absolute values for estimation results in Table 6 in Appendix A).

The absolute values of the optimized parameters and the computation time achieved on a single core with 2.4 GHz are given in Table 5. Additionally all values for R^2 are given there. While the model of Coulaloglou and Tavlarides (1977) and the extended model by Maaß and Kraume (2012) use the same term for the breakage probability (compare the exp-term in equation (5) and (6)) the value of $c_{2,b} = 3.3 \cdot 10^{-1}$ is the same in both approaches. The values are slightly higher a those reported in literature ($c_{2,b} = 1.1 \cdot 10^{-1}$ in the original publication by Coulaloglou and Tavlarides (1977)). This is true for all the estimated values and might be due to the fact, that the investigated system is breakage dominated.

Table 5 – parameter values after optimization

	computation time [s]	R^2 [-]	$c_{1,b}$	$c_{2,b}$	$c_{3,b}$
Coulaloglou and Tavlarides (1977)	2078	0.988	$2.2 \cdot 10^{-2}$	$3.3 \cdot 10^{-1}$	-
Maaß and Kraume (2012)	1961	0.987	$2.5 \cdot 10^{-3}$	$3.3 \cdot 10^{-1}$	-
Alopaeus et al. (2002)	2954	0.981	$1.2 \cdot 10^{1}$ $m^{2/3}s^{-1}$	$1.4 \cdot 10^{1}$	$2.0 \cdot 10^{-1}$
extended Alopaeus	2807	0.981	$4.0 \cdot 10^{-1}$ $m^{2/3}s^{-1}$	$2.9 \cdot 10^{-1}$	$2.0 \cdot 10^{-1}$

The results for the transient drop size distributions in comparison with the according simulations are given in Figure 4. The results for the point in time of 1, 10, 60 and 1170 min are shown. As the agitation time increases, the distributions shift to smaller drops. The agreements for all four approaches are quite convincing. Not only the mean diameter but also the shape of the distribution is reflected with all approaches. This is in good agreement with the results of Ruiz and Padilla (2004) who found almost no influence of the breakage rate on the shape of the distribution.

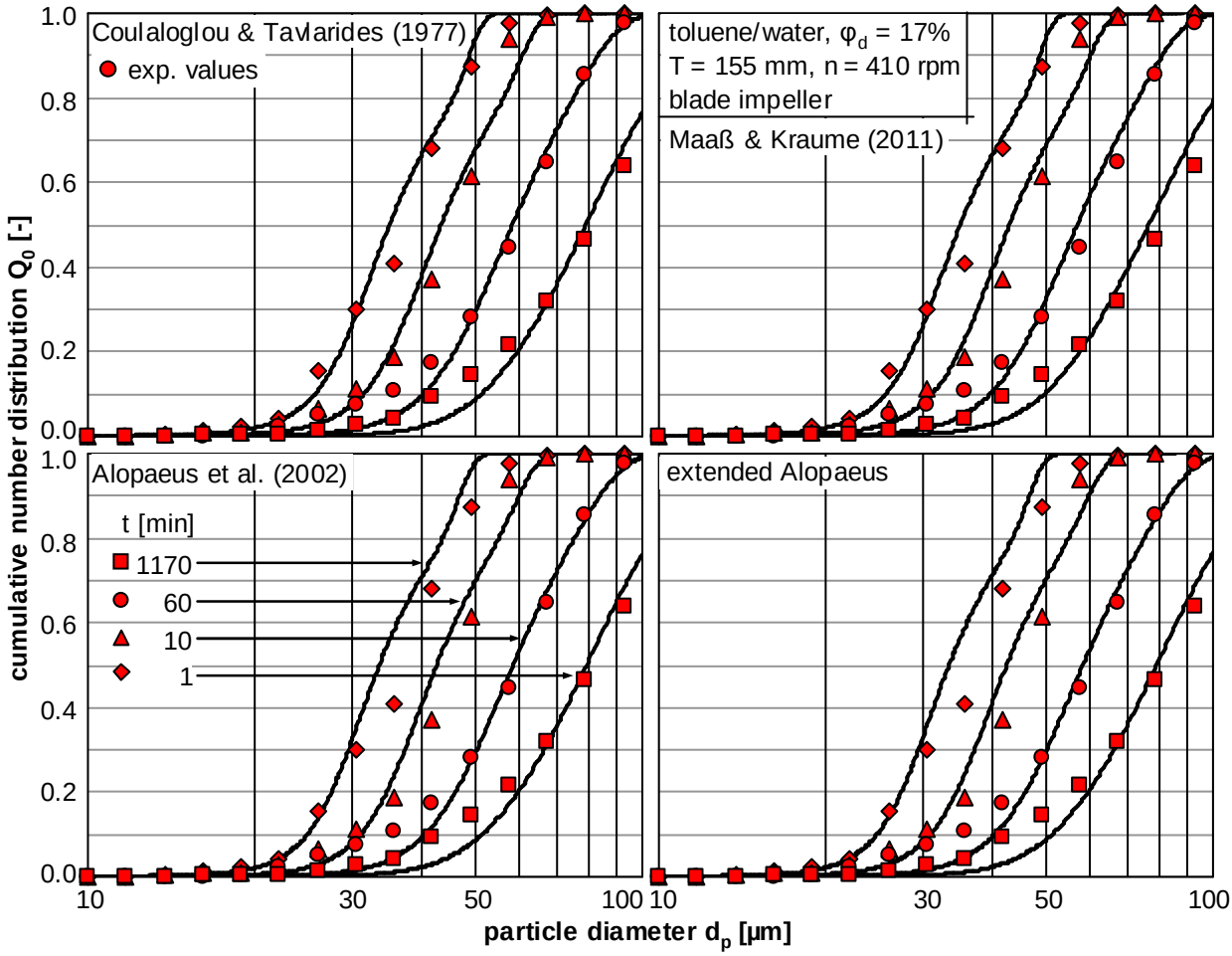

Figure 4 – simulated transient drop size distributions achieved by four different breakage rates after parameter estimation, compared with experiments

The last results presented in this section are the examination of the coalescence hindering. After the toluene/water system was agitated for 19.5 hours with a stirrer speed of 410 rpm, the stirrer speed was decreased to 250 rpm. The results for the transient Sauter mean diameters after the speed change are shown in Figure 5. The measurements were carried out for two more hours. During this period no size change was observed. All measured values scatter around the average value of 42.5 µm with a standard deviation of 1%. This proves the assumption that under the given circumstances, coalescence is completely hindered. Additionally this small experimental scattering proves the reliability and reproducibility of the measurements.

The drop size distribution after 1170 min of agitation with 410 rpm was used as initial distribution for all four breakage models and the drop size evolution with the lower stirrer speed was simulated. These values show no size decrease although the models are pure breakage models. Therefore, we can conclude that the parameters estimated for every model approach are relevant for different stirrer speeds. They do not overemphasize breakage as the coalescence test showed.

These estimated parameter values (see Table 5) were kept constant for every single model approach during the complete study.

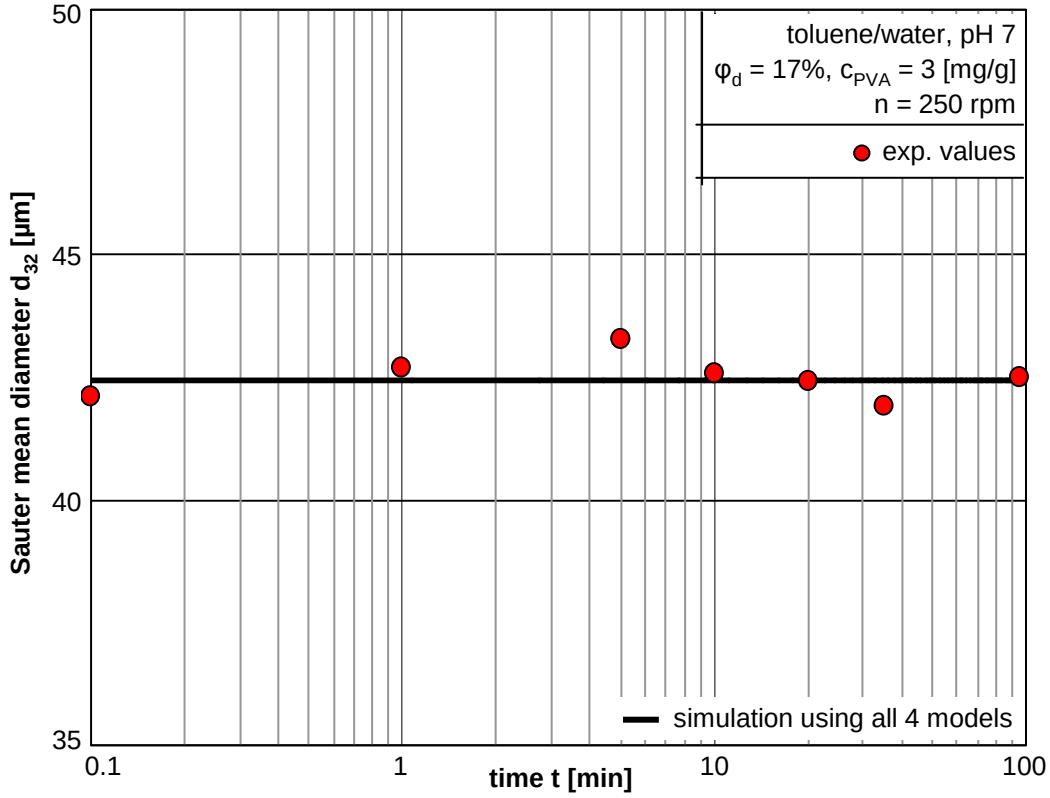

Figure 5 – transient Sauter mean diameter after significant decrease of the stirrer speed to examine coalescence hindering in the experiments and the simulations. All simulations were equal and fall into one curve.

5.3 Dispersed phase fraction

The influence of the dispersed phase fraction on the toluene/water system is shown in comparison to the simulation results by all four introduced breakage kernels in Figure 6. The results of d_{32} are shown for φ_d = 0.05, 0.2, 0.33 and 0.45 over a time of 60 min agitation.

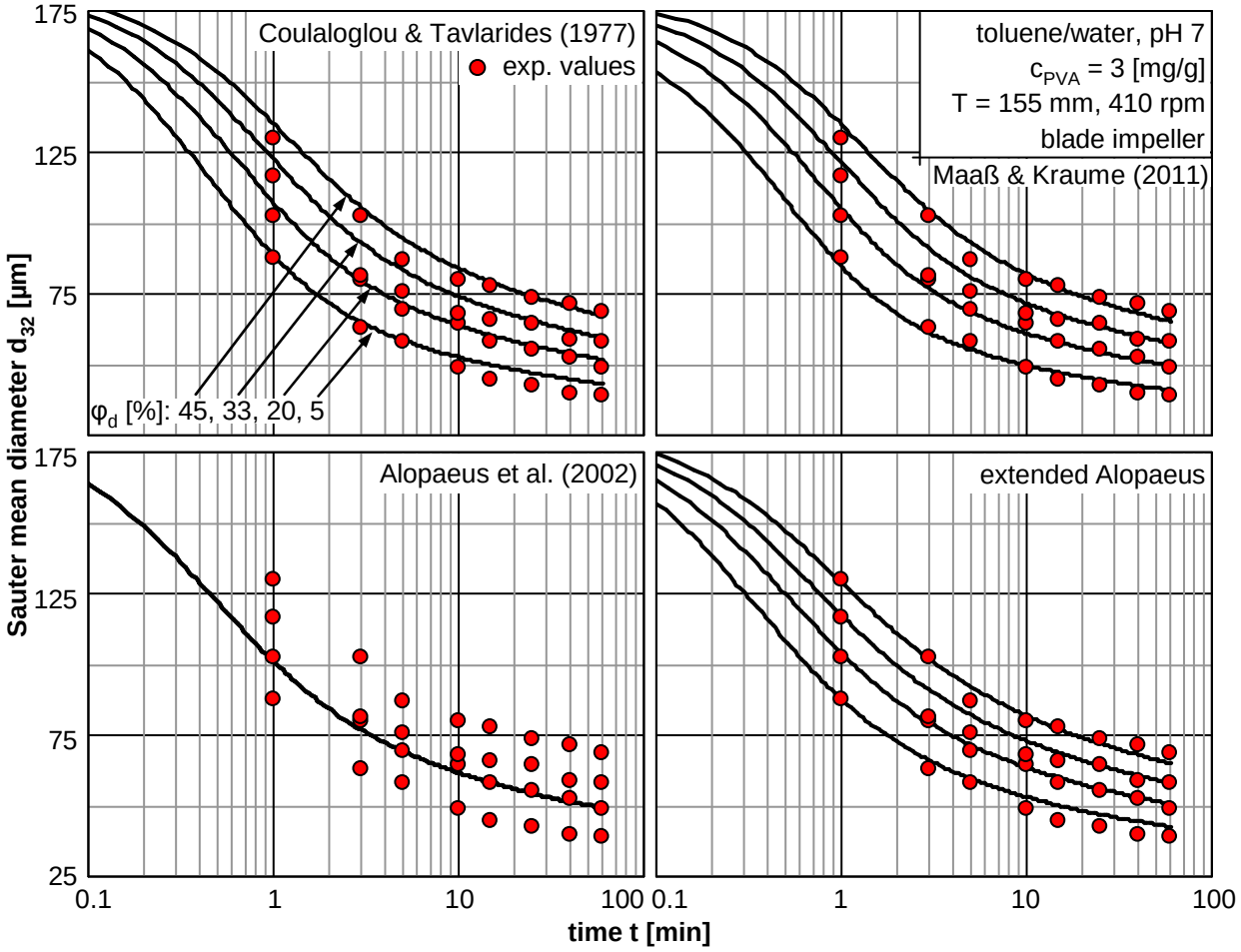

Figure 6 – Comparison of experiments (symbols) and simulations (lines) for the influence of dispersed phase fraction on transient Sauter mean diameter for the toluene/water system

Two major results can be observed. First, the experimental d_{32} strongly depends on the dispersed phase fraction for this non-coalescing system. The increase in hold-up leads to an increase in d_{32}, despite the absence of coalescence. This shows clearly the influence of the dispersed phase fraction on drop breakage. Secondly, the simulations are reflecting the influence of φ_d on d_{32} excellently, besides the model of Alopaeus et al. (2002).

The change in the viscosity of a turbulent medium causes a corresponding change in the average length scales of energetic eddies even at a constant level of external power input into the system. As viscosities of dilute and concentrated dispersions can differ due to differences in dispersed phase volumes (Doulah 1975), the viscosities of the dispersion used in this study have been measured. No influence of φ_d was found on the viscosity for the four investigated low viscous media. Therefore, the size increase can neither be related to increased coalescence as proposed by Delichatsios and Probstein (1976) nor to an increase in dispersion viscosity as proposed by Doulah (1975).

These conclusions show clearly that the hold-up should not only be considered via the mass balance, as in the model of Alopaeus et al. (2002), but should also directly affect the breakage models. If not, all simulations fall into the same curve as shown in Figure 6 with the results for the model of Alopaeus et al. (2002). The assumption that the turbulence is damped by an increase in

φ_d and that that can be expressed by a dampening of $\varepsilon^{1/3} \cdot (1+\varphi_d)^{-1}$ was supported through the presented results. The original model of Alopaeus et al. (2002) fails to predict the drop size change by changing φ_d. The slightly extended model approach (compare equation (7) and (8)) predicts the drop size change as a function of φ_d with outstanding precision.

A first conclusion can be drawn: The influence of the dispersed phase fraction on the drop sizes in breakage dominated systems can be well reproduced with PBE simulations. The breakage models require a turbulence damping factor $(1+\varphi_d)$, which is used in most of the common models.

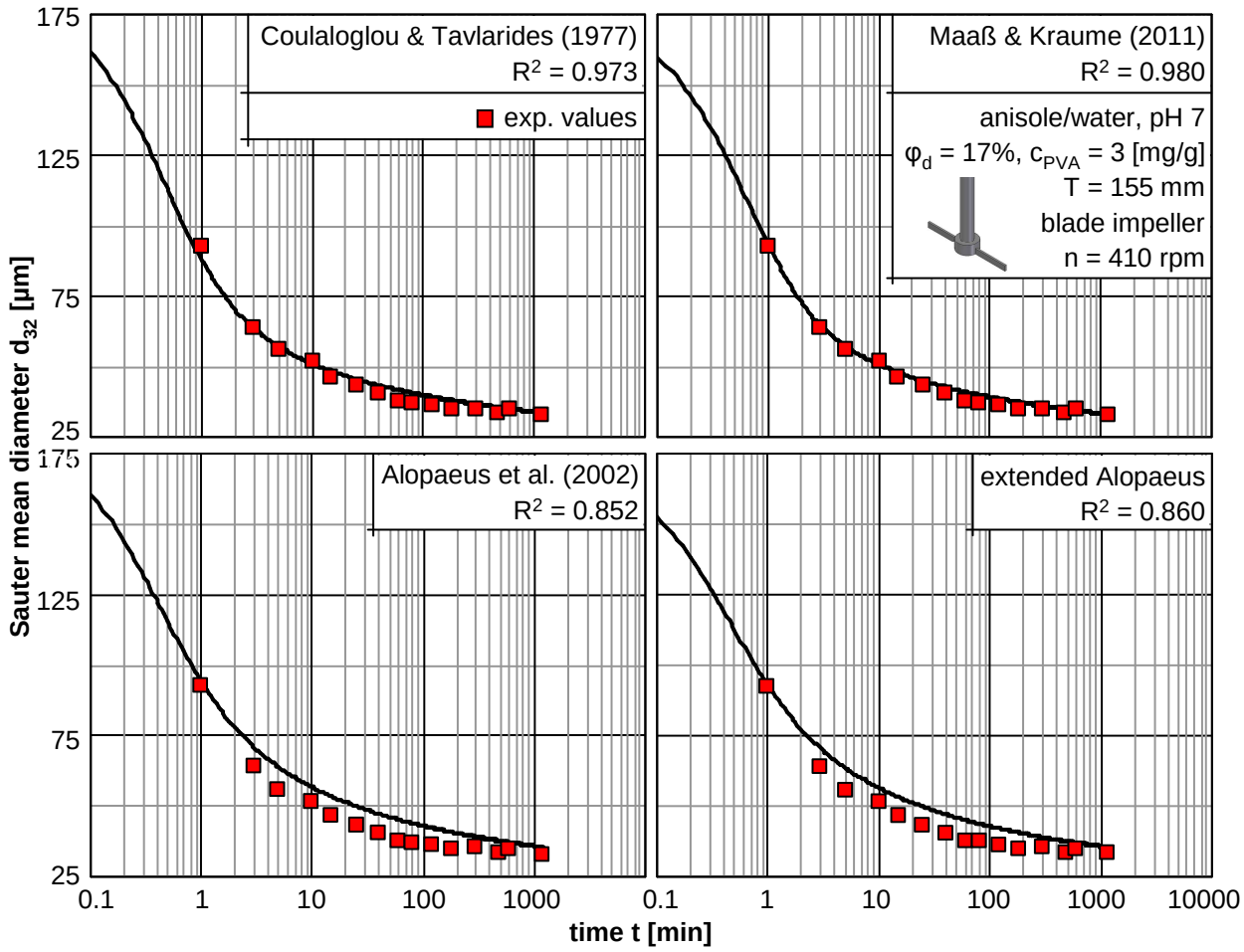

Figure 7 – experimental transient Sauter mean diameter for anisole/water system (symbols) compared with PBE simulations (lines)

The next step was to vary the hold-up for several liquid/liquid systems. The results for a long term experiment along with the one already discussed in Figure 3 are presented together with simulation results in Figure 7. The organic phase is now anisole while all other process parameters (continuous phase, φ_d, stirrer speed and set-up) were kept constant.

The interfacial tension for anisole/water was smaller than for toluene/water, but its viscosity is higher. These changes in the physical properties are well described by the model of Coulaloglou and Tavlarides (1977) and Maaß and Kraume (2012) using the same constants as for the toluene/water system. The other two simulation results based on the model of Alopaeus et al. (2002)

are less convincing. Although the simulations and the experiments were in the same size range (especially for the first and the last minute), the evolution of the size decrease is slower in the simulation than in the experiments. This is probably the influence of the higher viscosity. The increase in viscosity leads to a decrease in the breakage rate for the model of Alopaeus et al. (2002) (see equation (7)). This might be too strong for the investigated system and should be re-checked in further studies.

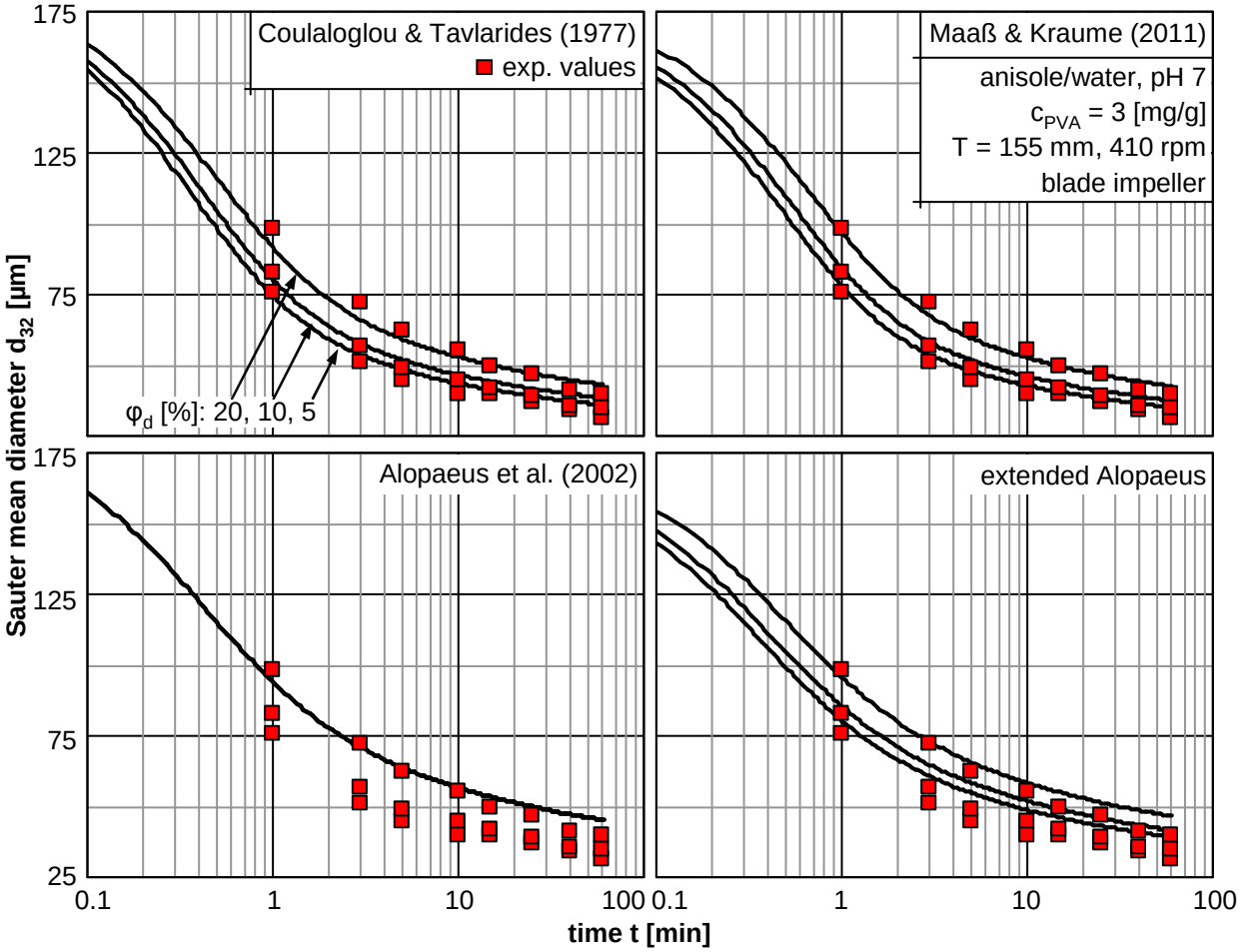

Figure 8 – influence of dispersed phase fraction on transient Sauter mean diameter for anisole/water compared with PBE simulations

In Figure 8 the results for three different dispersed phase fractions (φ_d = 0.05, 0.1 and 0.2) are given together with corresponding PBE simulations for the anisole/water system. The good agreements between predictions and measurements could be repeated for the model of Coulaloglou and Tavlarides (1977) and Maaß and Kraume (2012). The model of Alopaeus et al. (2002) fails as expected to predict the variation of drop sizes as a function of φ_d, as its extended version gives meaningful results for the tendencies. The absolute values are too large for the same reason as already discussed for the case with φ_d = 0.17 (see also Figure 7).

The results for the d_{32} over 60 min of agitation for the n-butyl chloride/water and the cyclohexane/water system are given in Figure 9. The higher interfacial tension of the cyclohexane/water

system leads to larger drops than the n-butyl chloride system. Additionally the higher viscosity of the cyclohexane compared to n-butyl chloride (see also the physical properties listed in Table 2) leads to more stable drops. The higher φ_d values always lead to larger drops for both systems.

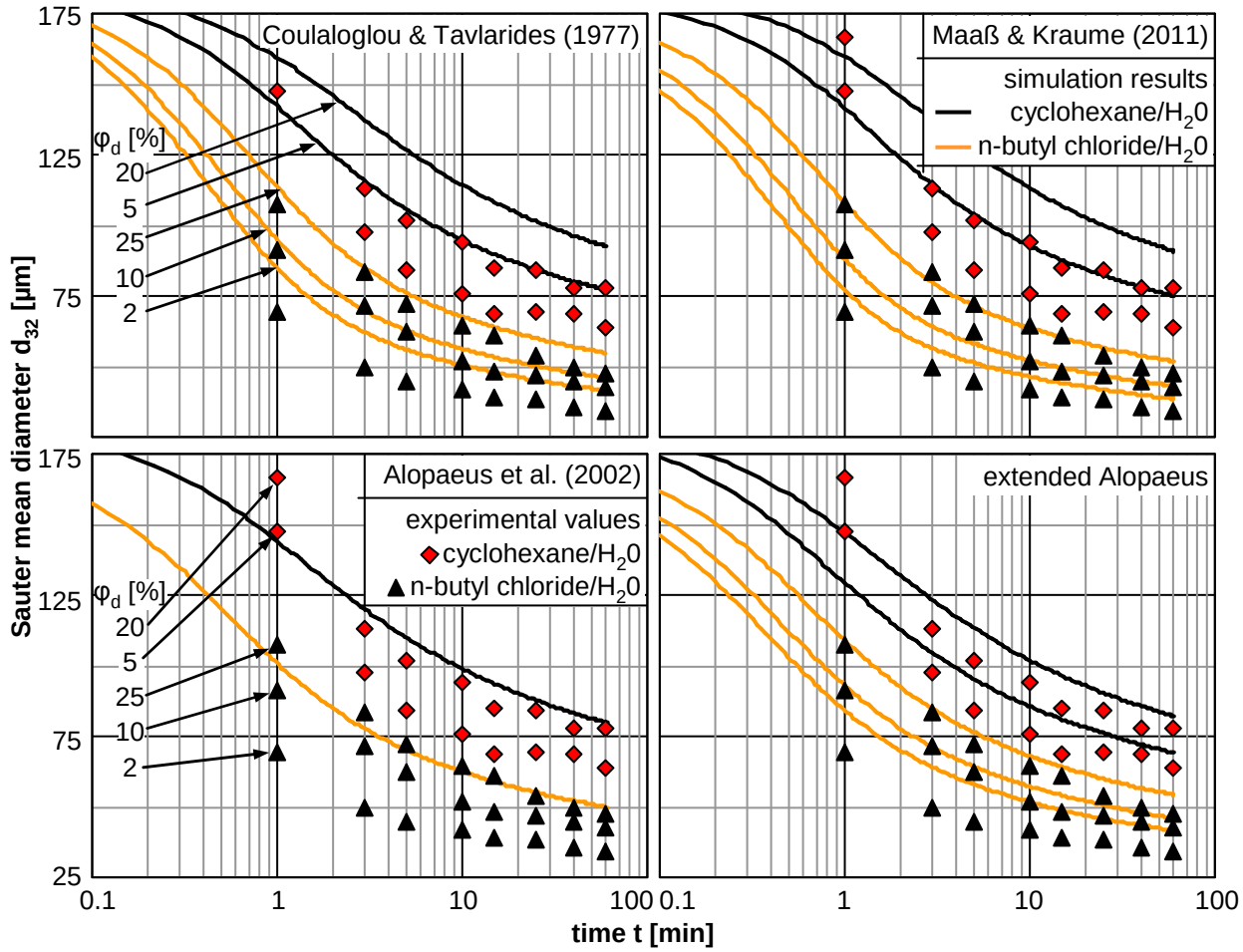

Figure 9 – transient Sauter mean diameter for different dispersed phase fractions of cyclohexane/water system (◊ symbols) and n-butylchloride/water system (▲ symbols) always compared with PBE simulations (lines)

The tendencies of the simulations reflecting the change in physical properties are acceptable for all four model approaches. The same is true for the change of φ_d, except for the results gained with the model of Alopaeus et al. (2002). This model and its simulation results will not be further discussed in this study, as it is not suitable for the prediction of the influence of φ_d.

The results for the transient d_{32} with the models of Coulaloglou and Tavlarides (1977) and Maaß and Kraume (2012) lead to too high values for the cyclohexane/water system. The models are underpredicting the evolution of the mean diameter. This is assumed to be based on an over emphasis of the influence of the interfacial tension in the models.

The evolution of the n-butyl chloride values were also underpredicted, but deviations between experiments and simulation are smaller compared to the cyclohexane/water system. This is especially true for the model by Maaß and Kraume (2012). The influence of the viscosity is consid-

ered in the breakage time by Maaß and Kraume (2012) but not by Coulaloglou and Tavlarides (1977). This advancement leads to more accurate prediction results.

For the n-butyl chloride/water system the same deviations between measurements and predicted values are found for the extended model of Alopaeus et al. (2002) as for the model of Coulaloglou and Tavlarides (1977). The prediction results for cyclohexane/water system are much better than for the other two model approaches.

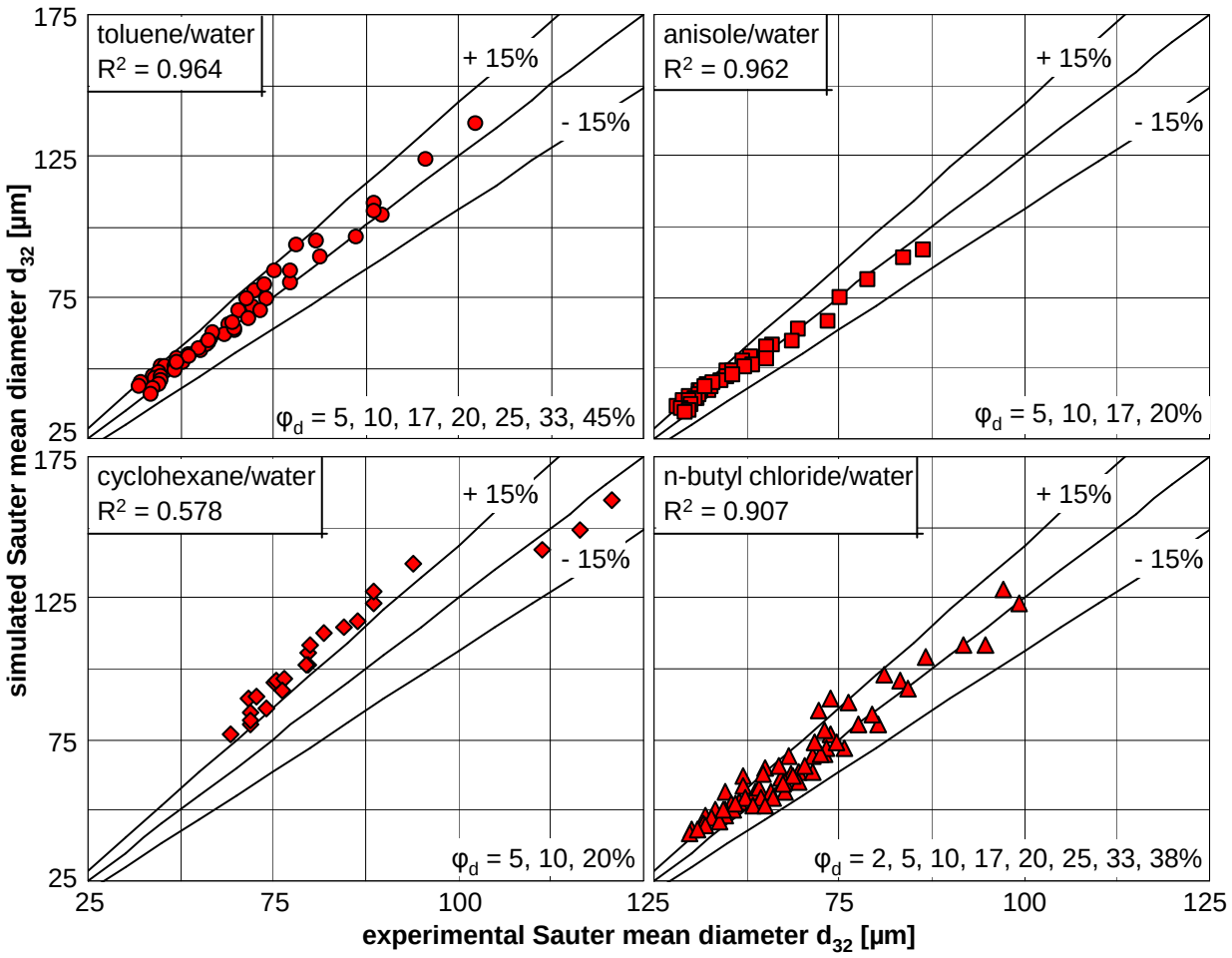

Figure 10 – parity plot evaluating the simulation results using breakage rate of Coulaloglou and Tavlarides (1977)

A clear evaluation is achieved by determining the coefficient of determination R^2 for all four liquid/liquid systems. The results are given in parity plots for the breakage model by Coulaloglou and Tavlarides (1977) (see Figure 10), Maaß and Kraume (2012) (see Figure 11) and the extended model of Alopaeus et al. (2002) (see Figure 12).

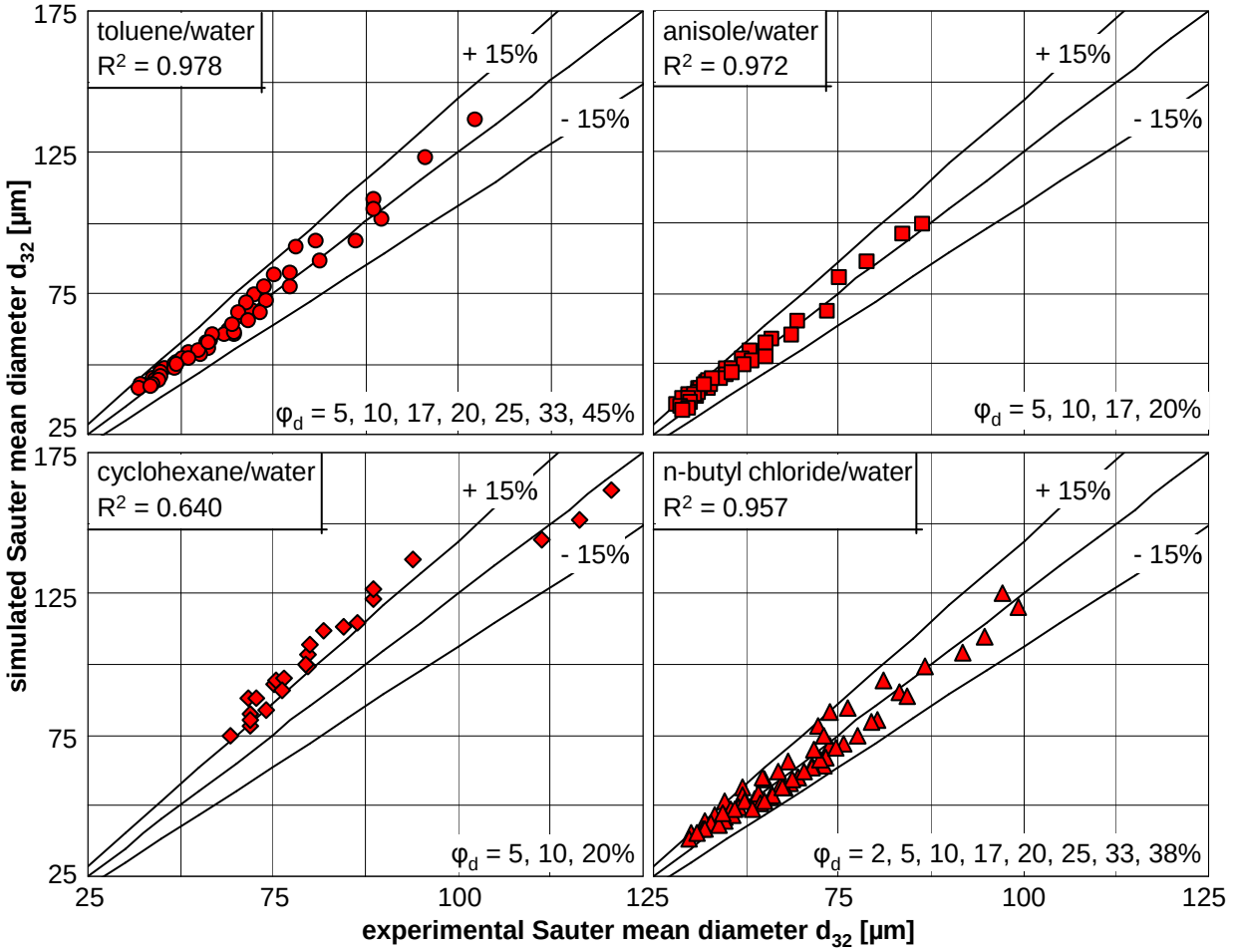

Figure 11 – parity plot evaluating the simulation results using breakage rate of Maaß and Kraume (2012)

The comparison between Figure 10 and Figure 11 clearly shows that the drop size evolutions of all four liquid/liquid systems are better described by the breakage model of Maaß and Kraume (2012) than by the model of Coulaloglou and Tavlarides (1977). The prediction results for the three systems (toluene/water, anisole/water, n-butyl chloride/water) are all on a high level of accuracy but the simulations with the model of Maaß and Kraume (2012) are always one to five percent more accurate. Both models show something between moderate and poor results for the cyclohexane/water system. Again the model of Maaß and Kraume (2012) is slightly better than the model of Coulaloglou and Tavlarides (1977) (R^2 = 0.640 compared to 0.578).

The prediction results with the extended Alopaeus model are different. Although the R^2 presented in Figure 12 are worse for three of the four systems compared to the results in Figure 10 and Figure 11, they are still moderate. The results for cyclohexane/water are much better compared to the values achieved with Coulaloglou and Tavlarides (1977) or Maaß and Kraume (2012). This shows the considerable promise of in this model approach. Further sensitivity analysis of the third parameter $c_{3,b}$ could reveal some additional fitting opportunities taking the viscous effects better into account. The last evaluation in this study will be based on the correlations also derived from the Hinze (1955) theory.

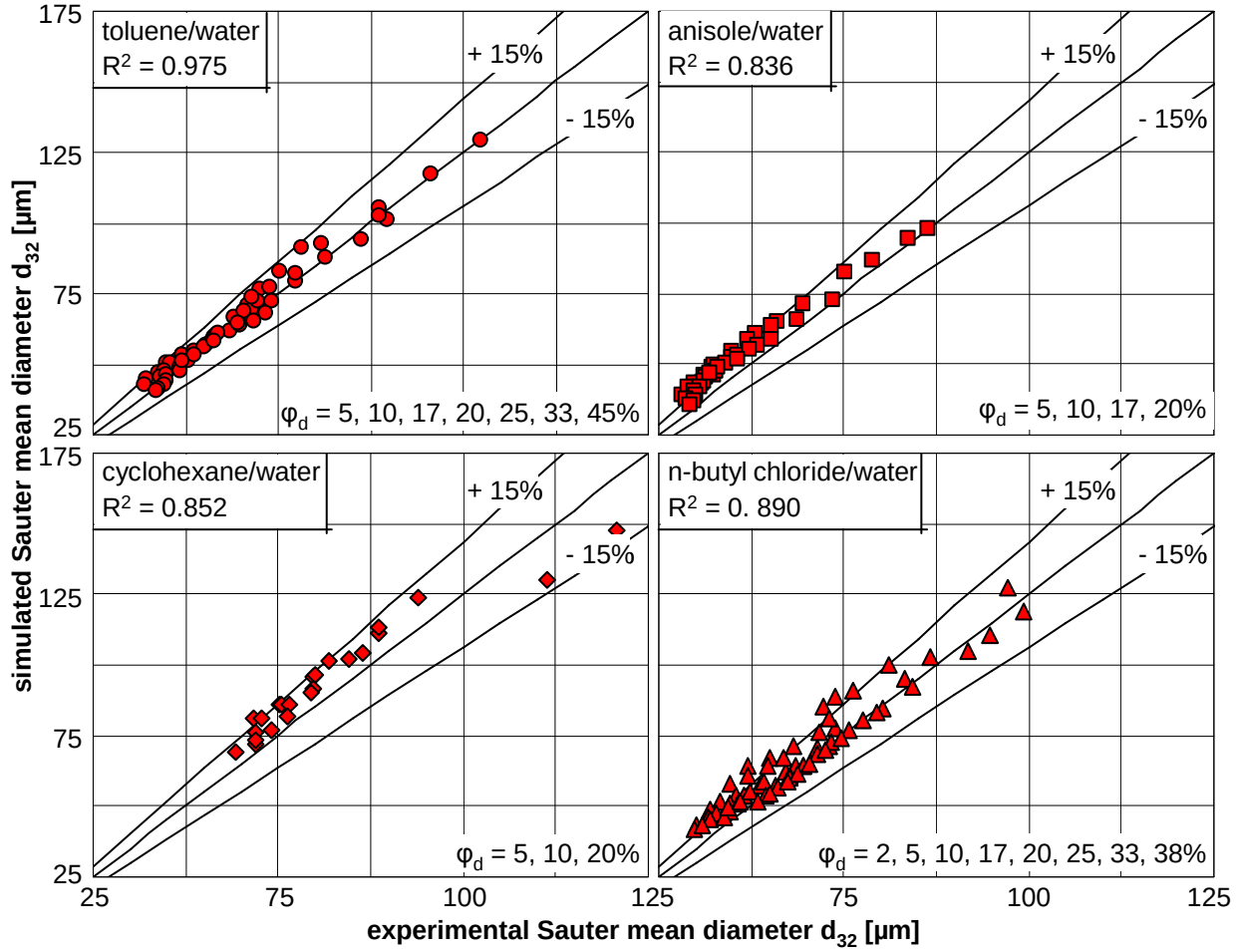

Figure 12 – parity plot evaluating the simulation results using extended breakage rate of Alopaeus et al. (2002)

Figure 13 shows the comparison between experimental Sauter mean diameter after 60 min of agitation and those calculated by equation (9). The experimental results show clearly that the effect of the dispersed phase fraction on the Sauter mean diameter is linear. The final correlation in terms of the Weber number is given by

$$\frac{d_{32}}{D} = 0.084 \cdot (1 + C_2 \varphi_d) We^{-0.6} \qquad (9)$$

The value for C_1 was set constant to 0.084 for all four investigated systems, as it stands for the geometrical parameters in the used system. It is in excellent agreement to the values used in literature. It is almost equal to the value determined by Coulaloglou and Tavlarides (1976). The little difference of 5% may be partly explained in terms of continuous vs. batch operation. Coulaloglou and Tavlarides (1976) were analyzing a continuously operated system.

The values for C_2 are all in the same range but different from each other. They are all above 0.96 which was stated as the possible maximum value for breakage dominated systems without any coalescence (Delichatsios and Probstein 1976). While the value is changing for the different non coalescing liquid/liquid systems, C_2 can not only be a coefficient describing the changing influence of coalescence. The extension of equation (9) with the use of the viscosity number following equation (2) did not lead to a more homogeneous description of the different systems. Still vari-

ous values for C_2, C_3 and C_4 need to be estimated to fit the correlations against the experimental values. A prediction with only one parameter combination was not possible for any of the results. Opposed to the correlation results, the population balances are not only able to give insights into and information about the evolution of the drop sizes in a turbulent system, but they are also more robust. A change in the investigated range of physical properties was predictable with moderate to excellent results.

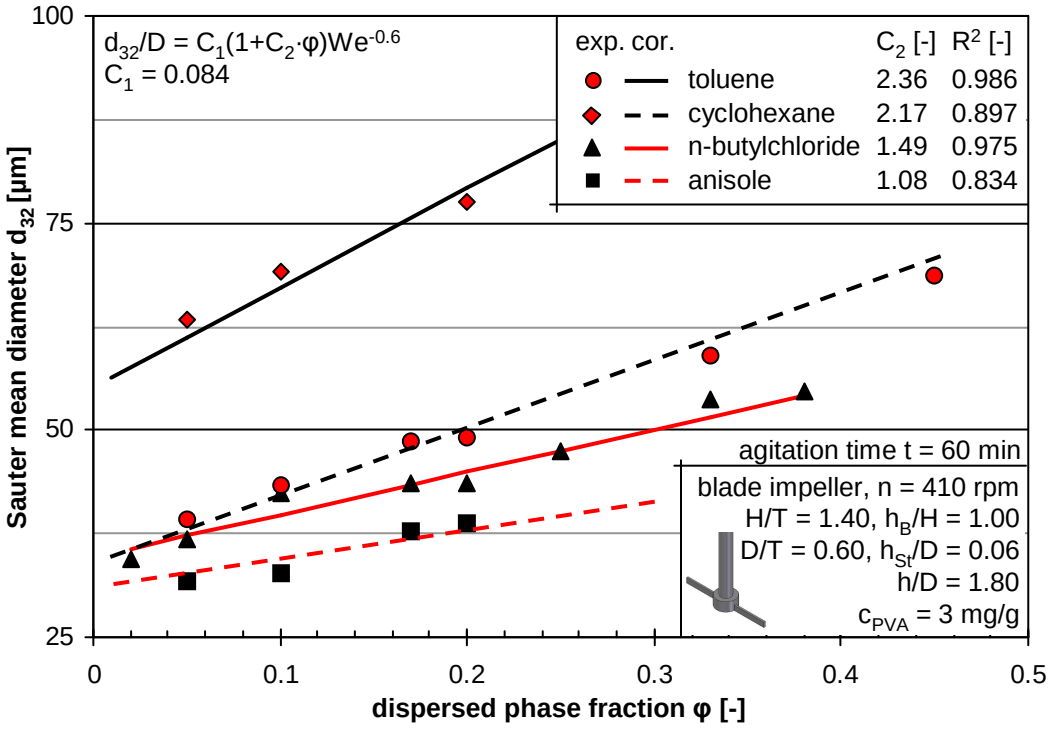

Figure 13 – Analysis of the prediction capacity of classical Weber correlation for varying dispersed phase fractions for four different liquid/liquid systems

6 CONCLUDING REMARKS

The effect of the dispersed phase fraction on the evolving drop size distribution in different low viscous liquid/liquid systems was investigated. The analysis focused on the drop breakage phenomena by hindering the coalescence completely. Therefore, polyvinyl alcohol concentrations were used around three times higher than the critical micelle concentration.

The measured drop sizes were decreasing along with agitation time and increasing with increasing dispersed phase fraction. As coalescence was completely hindered and also the measured viscosity showed no influence on the dispersed phase hold-up, the size increase is proposed to be a result of turbulence hindering.

This physical behavior was then estimated with different model approaches. On the one hand population balances were used to simulate the transient drop size development. On the other hand Weber number correlations were tested to reproduce the measured phenomena.

The influence of the dispersed phase fraction on the drop sizes in breakage dominated systems was well reproduced with PBE simulations. The used breakage models require a turbulence

damping factor ($1+\varphi_d$), which is used in most of the common models. Only the model of Alopaeus et al. (2002) failed to reproduce this influence scheme as it does not include any turbulence damping by the dispersed phase. The model constants have been fitted only once with only one set of experimental data from a toluene/water system

Summarizing the various PBE simulations we can conclude that the prediction of drop size in systems with different dispersed phase fractions can be easily predicted, if the model parameters are fitted to set of experiments studying the same species. The change of the physical system was successfully simulated with outstanding results for two of the three organics for the breakage model of Coulaloglou and Tavlarides (1977) and Maaß and Kraume (2012).

The Weber correlations were also able to reproduce the linear interdependency between the drop size and the dispersed phase fraction. Unfortunately, every change in the dispersed phase needed new parameter estimation. As at least three out of four different liquid/liquid systems were predicted with excellent results, the PBE is proposed as a more robust tool than the classical correlations widely used in academics and industries. Additionally, this kind of analysis allows insights not only into steady state behavior but also in the evolution of drop sizes.

ACKNOWLEDGEMENTS

This work was partly financially supported by the DFG through the Sonderforschungsbereich/Transregio 63 - project A6.

The authors gratefully acknowledge Ms. Miriam Bezeran Sauras, Ms. Susanne Buscher and Mr. Uli Dölchow for the excellent support with the experimental work. The supervision of the experiments by Andrea Hasselmann is gratefully acknowledged. The simulation work has been intensively supported by Ms. Beatriz Vazquez Pascual. Her help and joyful spirit during the project are gratefully acknowledged.

SYMBOLS

B - source term of breakage or coalescence [1/s]

c_i, C_i - numerical or correlation constants [various]

c - concentration

d - drop diameter [m]

d_{32} - Sauter mean diameter [m]

D - stirrer diameter [m]

D - sink term of breakage or coalescence [1/s]

g - breakage rate [1/s]

h - collision frequency [m/s]

h - bottom clearance, stirrer height [m]

l_B - baffle length [m]

H - liquid level [m]

n - stirrer speed [rpm]

Ne - Power or Newton number [-]

P - breakage probability [-]

t - time [s]

T - tank diameter [m]

V - volume [m^3]

We - Weber number

β - daughter drops size distribution

γ - interfacial tension [mN/m]

ε - energy dissipation rate [m^2/s^3]

η - dynamic viscosity [kg/(m·s)]

λ - coalescence efficiency [-]

ν - kinematic viscosity [m^2/s]

ν - number of daughter drops

ρ - density [kg/m^3]

φ - phase fraction [-]

SUBSCRIPTS

b - breakage

c - coalescence

c - continuous

crit - critical

d - dispersed

p - particle

st - stirrer

ABBREVIATIONS

C&T (1977) - Coulaloglou and Tavlarides (1977)

DDSD - daughter drop size distribution

M&K (2011) - Maaß and Kraume (2012)

PBE - population balance equation

PVA - polyvinyl alcohol

APPENDIX A

Table 6 – absolute values for and of the parameter estimation results

time [t]	Sauter mean diameter d_{32} [µm]				
	experiments	C&T (1977)	M&K (2011)	Alopaeus (2002)	ex. Alopaeus
1	104.7	103.36	103.32	101.26	101.19
3	70.4	75.54	74.15	76.79	76.65
5	68.1	67.50	66.31	69.47	69.32
10	62.1	60.02	59.02	61.96	61.46
15	57.4	56.66	55.57	58.36	57.91
25	52.7	53.32	52.44	54.50	54.35
40	50.9	50.60	49.95	51.66	51.30
60	48.7	48.60	48.01	49.27	49.12
80	48.5	47.33	46.77	47.87	47.71
120	45.0	45.70	45.19	46.07	45.91
180	44.9	44.24	43.78	44.44	44.28
300	44.2	42.58	42.18	42.61	42.45
550	42.6	41.21	40.86	41.09	40.94
1170	42.1	38.93	38.66	38.59	38.44

LITERATURE

Al Taweel, A.M. and Landau, J., 1977. Turbulence modulation in two-phase jets. Int. J Multiphase Flow, 3(4): 341-351.

Alexopoulos, A.H., Maggioris, D. and Kiparissides, C., 2002. CFD analysis of turbulence non-homogeneity in mixing vessels: A two-compartment model. Chem. Eng. Sci., 57(10): 1735-1752.

Alopaeus, V., Koskinen, J., Keskinen, K.I. and Majander, J., 2002. Simulation of the population balances for liquid-liquid systems in a nonideal stirred tank. Part 2 - Parameter fitting and the use of the multiblock model for dense dispersions. Chem. Eng. Sci., 57(10): 1815-1825.

Alopaeus, V., Moilanen, P. and Laakkonen, M., 2009. Analysis of stirred tanks with two-zone models. AIChE J., 55(10): 2545-2552.

Angle, C.W. and Hamza, H.A., 2006a. Drop sizes during turbulent mixing of toluene-heavy oil fractions in water. AIChE J., 52(7): 2639-2650.

Angle, C.W. and Hamza, H.A., 2006b. Predicting the sizes of toluene-diluted heavy oil emulsions in turbulent flow - Part 2: Hinze-Kolmogorov based model adapted for increased oil fractions and energy dissipation in a stirred tank. Chem. Eng. Sci., 61(22): 7325-7335.

Arai, K., Konno, M., Matunaga, Y. and Saito, S., 1977. Effect of Dispersed-Phase Viscosity on Maximum Stable Drop Size for Breakup in Turbulent-Flow. J. Chem. Eng. Jpn., 10(4): 325-330.

Azizi, F. and Al Taweel, A.M., 2010. Algorithm for the accurate numerical solution of PBE for drop breakup and coalescence under high shear rates. Chem. Eng. Sci., 65(23): 6112-6127.

Azizi, F. and Al Taweel, A.M., 2011. Turbulently flowing liquid-liquid dispersions. Part I: Drop breakage and coalescence. Chem. Eng. J., 166(2): 715-725.

Brown, D.E. and Pitt, K., 1972. Drop Size Distribution of Stirred Non-Coalescing Liquid-Liquid System. Chem. Eng. Sci., 27(3): 577-583.
Calabrese, R.V., Chang, T.P.K. and Dang, P.T., 1986. Drop Breakup in Turbulent Stirred-Tank Contactors .1. Effect of Dispersed-Phase Viscosity. AIChE J., 32(4): 657-666.
Chatzi, E.G., Boutris, C.J. and Kiparissides, C., 1991. Online monitoring of drop size distributions in agitated vessels: 2. Effect of stabilizer concentration. Ind. Eng. Chem. Res., 30(6): 1307-1313.
Chatzi, E.G. and Kiparissides, C., 1995. Steady-state drop-size distributions in high holup fraction dispersion systems. AIChE J., 41(7): 1640-1652.
Chen, Z., Prüss, J. and Warnecke, H.J., 1998. A population balance model for disperse systems: Drop size distribution in emulsion. Chem. Eng. Sci., 53(5): 1059-1066.
Cho, Y.G. and Kamal, M.R., 2002. Effect of the dispersed phase fraction on particle size in blends with high viscosity ratio. Polym. Eng. Sci., 42(10): 2005-2015.
Cohen, R.D., 1991. Effect of Turbulence Damping on the Steady-State Drop Size Distribution in Stirred Liquid Liquid Dispersions. Ind. Eng. Chem. Res., 30(1): 277-279.
Coulaloglou, C.A. and Tavlarides, L.L., 1976. Drop Size Distributions and Coalescence Frequencies of Liquid-Liquid Dispersions in Flow Vessels. AIChE J., 22(2): 289-297.
Coulaloglou, C.A. and Tavlarides, L.L., 1977. Description of Interaction Processes in Agitated Liquid-Liquid Dispersions. Chem. Eng. Sci., 32(11): 1289-1297.
Cull, S.G., Woodley, J.M. and Lye, G.J., 2001. Process selection and characterisation for the biocatalytic hydration of poorly water soluble aromatic dinitriles. Biocatal. Biotransform., 19(2): 131-154.
Delichatsios, M.A. and Probstein, R.F., 1976. Effect of Coalescence on Average Drop Size in Liquid-Liquid Dispersions. Ind. Eng. Chem. Fundam., 15(2): 134-138.
Doulah, M.S., 1975. Effect of Hold-up on Drop Sizes in Liquid-Liquid Dispersions. Ind. Eng. Chem. Fundam., 14(2): 137-138.
Einstein, A., 1906. Eine neue Bestimmung der Moleküldimensionen. Ann. Phys., 324(2): 289-306.
Einstein, A., 1911. Berichtigung zu meiner Arbeit: Eine neue Bestimmung der Moleküldimensionen. Ann. Phys., 339(3): 591-592.
El-Hamouz, A., 2009. Drop Size Distribution in a Standard Twin-Impeller Batch Mixer at High Dispersed-Phase Volume Fraction. Chem. Eng. Technol., 32(8): 1203-1210.
Gäbler, A., Wegener, M., Paschedag, A.R. and Kraume, M., 2006. The effect of pH on experimental and simulation results of transient drop size distributions in stirred liquid-liquid dispersions. Chem. Eng. Sci., 61(9): 3018-3024.
Galinat, S., Risso, F., Masbernat, O. and Guiraud, P., 2007. Dynamics of drop breakup in inhomogeneous turbulence at various volume fractions. J. Fluid Mech., 578: 85-94.
Godfrey, J.C., Obi, F.I.N. and Reeve, R.N., 1989. Measuring drop size in continuous liquid-liquid mixers. Chem. Eng. Prog., 85(12): 61-69.
Hinze, J.O., 1955. Fundamentals of the Hydrodynamic Mechanism of Splitting in Dispersion Processes. AIChE J., 1(3): 289-295.
Hoffmann, H. and Ulbricht, W., 1995. Faszinierende Phänomene in Tensidlösungen. Chem. unserer Zeit, 29(2): 76-86 (in German).
Jon, D.I., Rosano, H.L. and Cummins, H.Z., 1986. Toluene Water/1-Propanol Interfacial-Tension Measurements by Means of Pendant Drop, Spinning Drop, and Laser Light-Scattering Methods. J. Colloid Interface Sci., 114(2): 330-341.
Khakpay, A. and Abolghasemi, H., 2010. The Effects of Impeller Speed and Holdup on Mean Drop Size in a Mixer Settler with Spiral-Type Impeller. Can. J. Chem. Eng., 88(3): 329-334.
Kraume, M., Gäbler, A. and Schulze, K., 2004. Influence of physical properties on drop size distributions of stirred liquid-liquid dispersions. Chem. Eng. Technol., 27(3): 330-334.
Liao, Y. and Lucas, D., 2009. A literature review of theoretical models for drop and bubble breakup in turbulent dispersions. Chem. Eng. Sci., 64(15): 3389-3406.
Maaß, S., Gäbler, A., Zaccone, A., Paschedag, A.R. and Kraume, M., 2007. Experimental investigations and modelling of breakage phenomena in stirred liquid/liquid systems. Chem. Eng. Res. Des., 85(A5): 703-709.
Maaß, S., Metz, F., Rehm, T. and Kraume, M., 2010. Prediction of drop sizes for liquid-liquid systems in stirred slim reactors - Part I: Single stage impellers. Chem. Eng. J., 162(2): 792-801.

Maaß, S., Wollny, S., Voigt, A. and Kraume, M., 2011a. Experimental comparison of measurement techniques for drop size distributions in liquid/liquid dispersions. Exp. Fluids, 50(2): 259-269.
Maaß, S., Rehm, T. and Kraume, M., 2011b. Prediction of drop sizes for liquid-liquid systems in stirred slim reactors - Part II: Multi stage impellers. Chem. Eng. J., 168(2): 827–838.
Maaß, S., Eppinger, T., Altwasser, S., Rehm, T. and Kraume, M., 2011c. Flow field analysis of stirred liquid-liquid systems in slim reactors. Chem. Eng. Technol., 34(8): 1215-1227.
Maaß, S., Buscher, S., Hermann, S. and Kraume, M., 2011d. Analysis of particle strain in stirred bioreactors by drop breakage investigations. Biotechnol. J., 6(8): 979-992.
Maaß, S. and Kraume, M., 2012. Determination of breakage rates using single drop experiments. Chem. Eng. Sci., 70(3): 146-164.
Maaß, S., Rojahn, J., Hänsch, R. and Kraume, M., 2012. Automated drop detection using image analysis for online particle size monitoring in multiphase systems. Comp. Chem. Eng.(revised submitted): pp. 10.
Martínez-Bazán, C., Montanés, J.L. and Lasheras, J.C., 1999. On the breakup of an air bubble injected into a fully developed turbulent flow. Part 1. Breakup frequency. J. Fluid Mech., 401: 157-182.
Narsimhan, G., Gupta, J.P. and Ramkrishna, D., 1979. Model for Transitional Breakage Probability of Droplets in Agitated Lean Liquid-Liquid Dispersions. Chem. Eng. Sci., 34(2): 257-265.
Nienow, A.W., 2004. Break-up, coalescence and catastrophic phase inversion in turbulent contactors. Adv. Colloid Interface Sci., 108: 95-103.
Okufi, S., Perez De Ortiz, E.S. and Sawistowski, H., 1990. Scale-up of liquid-liquid dispersions in stirred tanks. Can. J. Chem. Eng., 68(3): 400-406.
Pacek, A.W., Man, C.C. and Nienow, A.W., 1998. On the Sauter mean diameter and size distributions in turbulent liquid/liquid dispersions in a stirred vessel. Chem. Eng. Sci., 53(11): 2005-2011.
Patruno, L.E., Dorao, C.A., Svendsen, H.F. and Jakobsen, H.A., 2009. Analysis of breakage kernels for population balance modelling. Chem. Eng. Sci., 64(3): 501-508.
Raikar, N.B., Bhatia, S.R., Malone, M.F. and Henson, M.A., 2009. Experimental studies and population balance equation models for breakage prediction of emulsion drop size distributions. Chem. Eng. Sci., 64(10): 2433-2447.
Razzaghi, K. and Shahraki, F., 2010. On the effect of phase fraction on drop size distribution of liquid-liquid dispersions in agitated vessels. Chem. Eng. Res. Des., 88(7A): 803-808.
Ruiz, M.C. and Padilla, R., 2004. Analysis of breakage functions for liquid-liquid dispersions. Hydrometallurgy, 72(3-4): 245-258.
Sathyagal, A.N. and Ramkrishna, D., 1996. Droplet breakage in stirred dispersions. Breakage functions from experimental drop-size distributions. Chem. Eng. Sci., 51(9): 1377-1391.
Scott, L.S., Hayes, W.B. and Holland, C.D., 1958. The Formation of Interfacial Area in Immiscible Liquids by Orifice Mixers. AIChE J., 4(3): 346-350.
Sengupta, B., Sengupta, R. and Subrahmanyam, N., 2006. Process intensification of copper extraction using emulsion liquid membranes: Experimental search for optimal conditions. Hydrometallurgy, 84(1-2): 43-53.
Singh, K.K., Mahajani, S.M., Shenoy, K.T. and Ghosh, S.K., 2008. Representative drop sizes and drop size distributions in A/O dispersions in continuous flow stirred tank. Hydrometallurgy, 90(2-4): 121-136.
Singh, K.K., Mahajani, S.M., Shenoy, K.T. and Ghosh, S.K., 2009. Population balance modeling of liquid-liquid dispersions in homogeneous continuous-flow stirred tank. Ind. Eng. Chem. Res., 48(17): 8121-8133.
Tsouris, C. and Tavlarides, L.L., 1994. Breakage and coalescence models for drops in turbulent dispersions. AIChE J., 40(3): 395-406.
Wulkow, M., Gerstlauer, A. and Nieken, U., 2001. Modeling and simulation of crystallization processes using parsival. Chem. Eng. Sci., 56(7): 2575-2588.
Zerfa, M. and Brooks, B.W., 1996. Prediction of vinyl chloride drop sizes in stabilised liquid-liquid agitated dispersion. Chem. Eng. Sci., 51(12): 3223-3233.